

# Improvements in the Reliability and Efficiency of Body-fitted Cartesian Grid Method

Keiichiro Fujimoto<sup>1</sup>

*JAXA's Digital Innovation Center, JAXA, Sagamihara, Kanagawa, 229-8510, Japan*

Kozo Fujii<sup>2</sup>

*Institute of Space and Astronautical Science, JAXA, Sagamihara, Kanagawa, 229-8510, Japan*

*and*

Z. J. Wang<sup>3</sup>

*Department of Aerospace Engineering, Iowa State University, Ames, IA 50011*

**In order to improve efficiency of the body-fitted Cartesian grid method and to make it possible to apply a geometry which includes complicated features such as small gaps, an extruded ghost surface is utilized. In the proposed approach, the grid front is generated by Cartesian grid generation over the ghost surface instead of the near-surface cell removal, which results in the faster turnaround and the flexibility to handle complicated geometry. By controlling length of an extrusion displacement vector, layer grid thickness, and by controlling grid resolution in a effective way such as sphere-type sources, an arbitrarily-shaped grid front can be obtained. As a result of this flexible capability to generate the arbitrarily-shaped grid front, body-fitted Cartesian grid method has been successfully extended to handle narrow gap problems.**

## I. Introduction

Since an aerodynamic discipline is one of the dominant factors in the conceptual design of space transportation systems, wide range of aerodynamic analysis is required to obtain the aerodynamic data and to understand the flow mechanisms. Since vehicle's flight trajectory is directly influenced by its aerodynamic characteristics, an aerodynamic analysis should be performed with sufficient accuracy even in the early design stages. In addition, tremendous numbers of design variables should be considered such as fuselage, wing shape, aerodynamic fins and so on, and resulting airframe becomes complicated in shape. In addition, the free-stream dynamic pressure is larger especially under the subsonic and transonic speed regime and the vehicle's aerodynamic characteristics shows non-linear behavior due to the viscous-effect-dominant flows. Thus, the viscous flow computation is essential even in early design stages. In addition wide variety of aerodynamic prediction should be done under various flow conditions. In order to achieve promising aerodynamic design by exploring wide range of design space, rapid and still accurate aerodynamic analysis method is crucial.

Currently, development activities of next generation expendable launch vehicles are under way at Japan Aerospace Exploration Agency (JAXA). In addition, conceptual study of reusable launch vehicle is also in progress. As mentioned above aerodynamic design is key issue for successful development of space transportation systems. An establishment of the rapid and still accurate aerodynamic analysis method for the use in early design stage is the final goal of this study. The method should have capability to handle high Reynolds number turbulent viscous flow over complicated geometry.

---

<sup>1</sup>Aerospace Project Research Associate, JAXA's digital Innovation Center, JAXA, AIAA member

<sup>2</sup>Professor, Department of Space Transportation Division, AIAA Fellow

<sup>3</sup>Associate Professor of Aerospace Engineering, Iowa State University, Associate Fellow of AIAA

Computational fluid dynamics (CFD) has superior advantages for the use in the early design stage. Therefore, CFD analysis has been widely utilized in many practical design applications. Especially in case of the high Reynolds number viscous flow over the complicated geometries, unstructured prismatic/tetrahedral hybrid grid method<sup>1-3</sup> has been matured as a most promising approach in the last twenty years. However, since the layer grid generation over the complicated geometry still requires an experience of the specialist and long working time. Flow structures such as shock waves, flow separation pattern change with the flow conditions. In order to estimate aerodynamic characteristics accurately, enough grid points should be distributed in the important flow structure area. When parametric aerodynamic study is performed by using unstructured hybrid grid method, the computational grid should be re-generated respectively for each flow condition due to the difficulty of solution adaptive mesh refinement. It is too expensive to use in the early design stages. While structured over-set grid method is also established approach to tackle high Reynolds number viscous flows<sup>4</sup>. For our purpose, it is also too expensive for the use in early design stages of space transportation system.

While, there has been a renewed interest in using Cartesian grids for complicated geometries. Cartesian grid-based approach has superior advantages for the use in early design stages such as short turnaround, accuracy, and favorable usability requiring less expertise as comparing with hybrid grids. In last decade, continuing research effort has been made to extend Cartesian grid method for the high Reynolds number viscous flow computations. Many preferable advantages of Cartesian-grid based viscous flow computation are reported such as geometrical flexibility, capability of solution adaptive grid refinement, and efficiency of filling three dimensional space<sup>5-17</sup>. These are strong advantages to achieve rapid and still accurate aerodynamic analysis method for an aerodynamic study in early design stage. In Fig. 1, CFD technology map for aerodynamic analysis of launch vehicle is shown, in which vertical axis shows turnaround time and horizontal axis shows accuracy of the computed result. Our target is to establish the aerodynamic analysis method whose accuracy is same as structured over-set, which can handle complicated geometry same as unstructured hybrid grids and much less expensive than all others. There exit two approaches for the Cartesian grid-based viscous flow computation as shown in Fig. 2. One is “Hybrid grid approach” in which prismatic layer grid is used to resolve surface shape, the other is “Body-fitted Cartesian grid approach” in which the layer grid is generated by the projection of the grid front as shown in right of Fig. 2. Although Cartesian grid-based over-set method is suitable for moving body problem, the discontinuous interface appears between layer and volume cells, it is difficult to use the computational grid for other purpose rather than CFD such as structural analysis and so on. Therefore, body-fitted Cartesian grid method was selected and studied to establish the rapid and still accurate aerodynamic analysis method in the present authors’ previous studies<sup>13, 14</sup>. In the body-fitted Cartesian grid method, layer grid is generated by the projection of grid front onto the surface. Thus, surface grid is resulting in the foot print of the grid front. There exist various geometrical features in the airframe

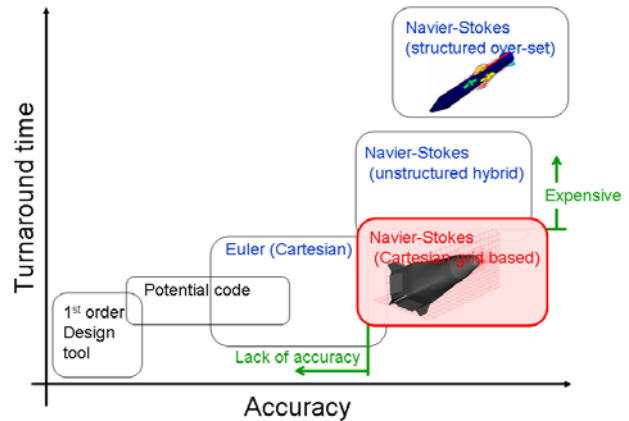


Figure 1. CFD technology map for engineering design.

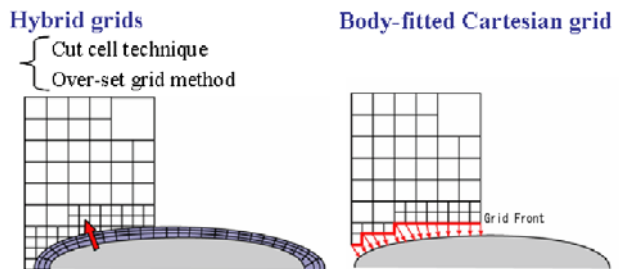


Figure 2. Cartesian grid-based viscous flow computations.

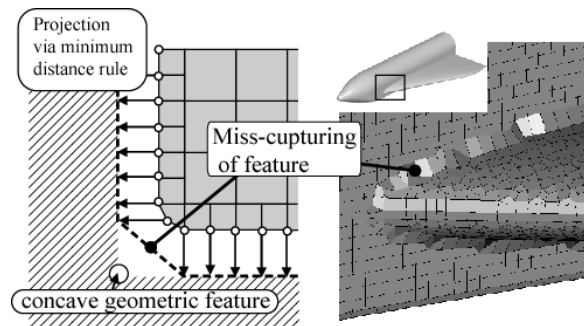


Figure 3. Projection of the Cartesian grid front nodes via minimum distance rule.

shape such as trailing edge line and wing and fuselage joint. These features should be resolved by surface grid nodes. Without any treatment, geometrical features are not resolved with the surface grid as shown in right of Fig. 3. In order to preserve features, optimization-based feature capturing method was developed in the present authors' past study<sup>17</sup>. It was clarified that the method is robust to capture various types of geometrical features.

In this study, further improvements in robustness and an efficiency of computational grid are pursued. Objectives of this study are following.

(Objective 1) An improvement of efficiency for the grid front generation

(Objective 2) Development of explicit grid resolution control method

(Objective 3) Extension of body-fitted Cartesian grid method to narrow gap geometry

In section II, process overview of body-fitted Cartesian grid method is described and background for each objectives are also given. In section III, technique to improve efficiency of grid front generation is discussed. In section IV, explicit grid resolution control method is discussed. In section V, technique to extend body-fitted Cartesian grid method to narrow gap problem is discussed. Finally the paper is concluded with the discussion on demonstration cases in section VI.

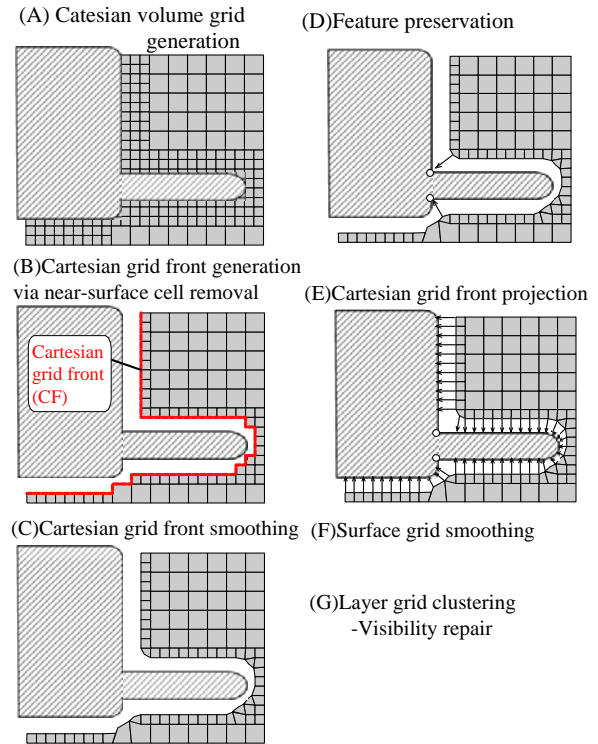


**Figure 4. Body-fitted Cartesian grid method process.**

## II. Body-fitted Cartesian Grid Method

In Fig. 4, overview of the procedure of body-fitted Cartesian grid method is shown. Initially A) Cartesian grid is generated over the body, and B) the near-surface Cartesian cells are removed to obtain the Cartesian grid front (CF) which covers the body. Then, C) CF is smoothed by using Laplace-type equation. Before the projection of CF, D) successive grid nodes on CF are selected to capture geometric features. Finally E) the smoothed CF is projected onto the surface to obtain single layer cell. In order to improve grid quality, F) surface grid is smoothed. In order to resolve viscous boundary layer flow, G) single layer grid is clustered in the normal direction.

### Background of objective 1

Since near-surface cell removal is based on the distance between cell nodes and the surface, this operation requires time-consuming closest point search for each candidate near-surface Cartesian cells. Computational time for step B) is almost half of the total required time. In the grid generation for DLR-F6 wing-body model, when geometry element number is 97942 and number of resulting volume Cartesian cell is 72759, total turnaround time is about 12 minutes, while required time for Cartesian front generation is about 5 minutes by using DELL precision 670 whose CPU is Xeon 2.8 GHz. Since required time for closest point search is proportional to the number of geometry element number, if number of element number becomes large situation becomes worse. In section III, technique to improve efficiency of grid front generation is discussed.

### Background of objective 2

In the generation of initial volume Cartesian cells, geometric adaptive grid refinement technique is used to refine intersected cell (cut cell). For each refinement step, cell level gap between the Cartesian cell and neighbor cell is monitored not to be more than one. Therefore, by this treatment cells surrounding refined cell are also refined as shown in Fig. 5. By specifying large cell level for geometric adaptive grid refinement, the volume cell resolution can be controlled. However, specification of large cell level might result in the excessive number of cells. Since Cartesian grid can be easily refined, more straightforward and explicit technique to control volume cell resolution is developed and discussed in section IV.

### Background of objective 3

In the design of space transportation system, the geometries with the narrow gap such as high lift devices, rocket engine nozzle and body joint should be considered. In body-fitted Cartesian grid method, the body should be covered entirely with the Cartesian grid front to obtain valid layer grid. Therefore, during removal of near-surface cell in the narrow gap region, special treatment is taken for the distance of the removal. Without any treatment, the grid front results in the undesirable situation as shown in right of Fig. 6. Key issue to handle narrow gaps with body-fitted Cartesian grid method is how to obtain valid Cartesian grid front which covers body entirely as shown in left of Fig.6. Technique to handle narrow gap problem is discussed in section V.

### III. Efficiency Improvement of Grid Front Generation

In the present authors' past studies<sup>13,14</sup>, in order to obtain Cartesian grid front, near-surface Cartesian cells are removed based on the distance from the body surface. Since this process requires closest point search between each cell vertex and numerous triangle surface elements, it takes long time to finish this process. In Table 1, breakdown of processing time for grid generation over rocket geometry is shown. For this problem, workstation PC with Intel (R) Xeon CPU 2.8 GHz is used. Geometry input file has 161760 triangle elements, and resulting volume grid consists of about 487000 cells. As shown in Table. 1, processing time for Cartesian grid front generation is about half of total. This processing time becomes larger as the number of removal cell and surface triangle elements increase. In order to reduce this processing time, new Cartesian grid front generation method is proposed in the present study as shown in Fig. 7. By extruding input surface outward based on the normal vector on the surface nodes, ghost surface is generated as shown in (A) of Fig. 7. Then, the volume Cartesian grid is generated over this ghost surface. Since there is distance between input and the ghost surface, the layer grid can be generated in this space. In the present method, the Cartesian grid front is obtained simply by generation of Cartesian grid over the ghost surface. Processing time for Cartesian grid front generation is remarkably reduced. As shown in Table. 1, it takes 5 minutes to obtain Cartesian grid front by using the present method, which is three times faster than the original method. It should be noted that most of the processing time is computation time, human time is very small which is less than 10 % of

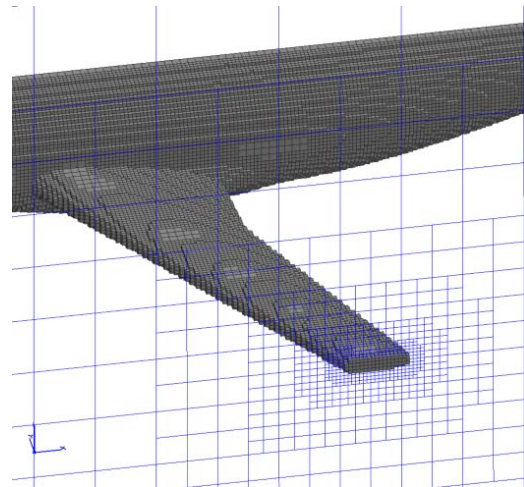


**Figure 5. Cartesian grid front and sectional view of Cartesian grid over DLR-F6 wing-body model .**

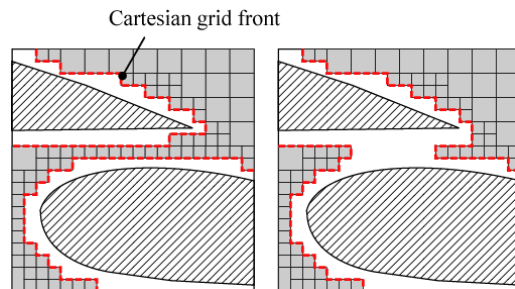


**Figure 6. Invalid grid front generated for high-lift device.**

total. Though it is effective to parallelize the code, the present code has not been parallelized yet. Computational time can be reduced future work of parallelization and improvement of a computer performance.

Since this distance corresponds to the layer grid thickness, layer grid thickness can be controlled by changing displacement vector length for the surface extrusion. This ghost surface is used also for the narrow gap treatment will be discussed in section V. Ghost surface and Cartesian cells generated for DLR-F6 wing-body model are shown in Fig. 8.

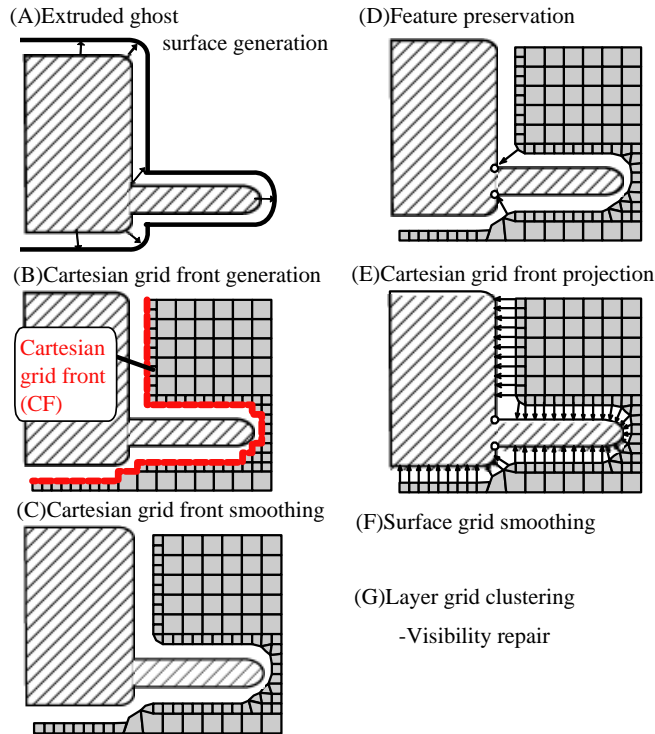


Figure 7. New body-fitted Cartesian grid method based on the ghost surface.

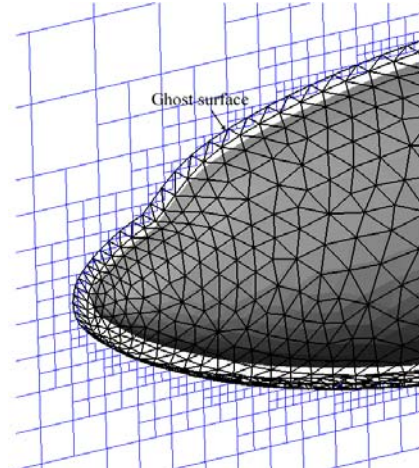


Figure 8. Ghost surface and Cartesian grid generated for DLR-F6 wing-body model.

Table 1. Processing time comparison for body-fitted Cartesian grid generation for rocket geometry.

	Original approach	Present
(A) Cartesian volume grid generation	8min 20sec (25.6%)	9min (40.6%)
(B) Cartesian grid front (CF) generation via near-surface cell removal	<b>16min (49.2%)</b>	<b>5min (22.6%)</b>
(C) CF smoothing	30sec (1.5%)	30sec (2.3%)
(D) Feature preservation	2min 10sec (6.7%)	2min 10sec (9.8%)
(E) Initial Surface grid generation via CF projection	2min 30sec (7.7%)	2min 30sec (11.3%)
(F,G) Layer Grid generation	3min (9.2%)	3min (13.5%)
Total	32min 30sec	22min 10 sec

#### IV. Explicit Grid Resolution Control

In body-fitted Cartesian grid method resulting surface grid corresponds to the footprint of Cartesian grid front, the grid resolution is controlled by the refinement of Cartesian cells in the Cartesian grid front generation process. Since it is easy to refine the Cartesian cells, straight forward and explicit grid resolution control method can be used. In the present study, sphere-type surface and volume sources are used as shown in Fig. 9. By specification of the center coordinate and radius, sphere can be defined in the computational space. For each sphere source, desired cell level or length scale is specified as the grid resolution control parameter. In case of volume source, Cartesian cell inside the sphere is refined until the cell level reaches specified cell level as shown in left of Fig. 9. In case of surface source, Cartesian cut cell which intersects with body inside the sphere will be refined as shown in right of Fig. 9.

This grid resolution control method is simple but powerful when the sphere center coordinates are given in the effective way. One of the examples for effect of the sphere source is shown in Fig. 10. In this example, sphere-type volume sources are generated along the feature line. As a result, Cartesian grid front facets near the feature line are smaller than others. Consequently, corresponding surface grid facets are also smaller as shown in right of Fig. 10.

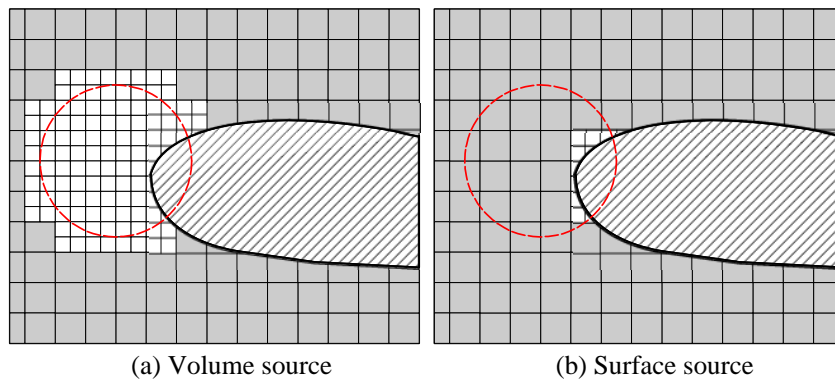


Figure 9. Sphere-type volume source and surface source to control grid resolution.

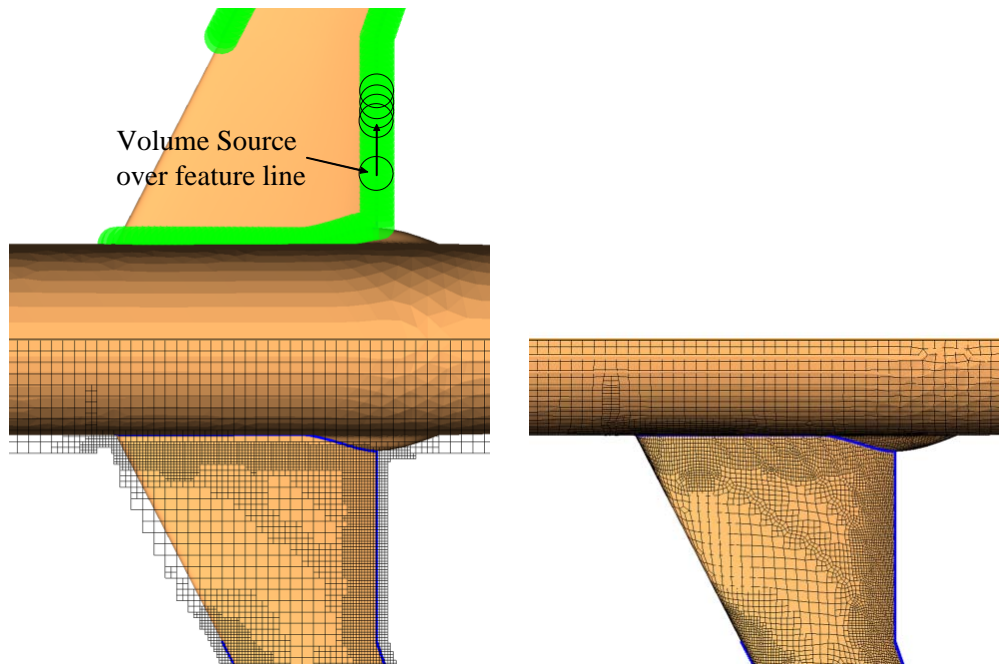
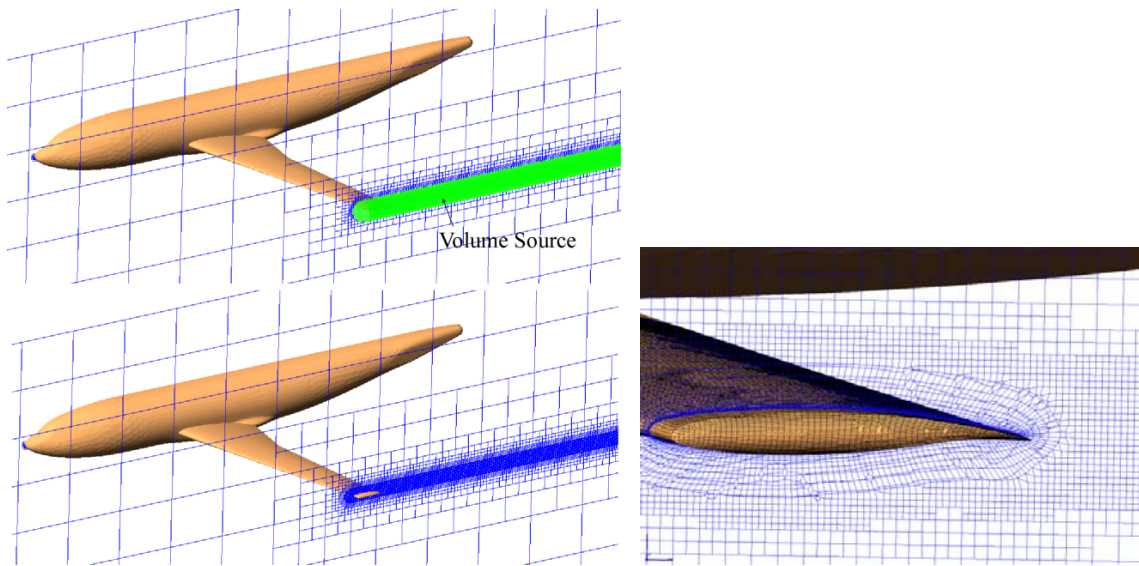


Figure 10. Sphere-type volume source and generated Cartesian grid front for DLR-F6 wing-body model (left: Volume source and Cartesian grid front. right: surface grid).

In the computational grid generation by usual prismatic/tetrahedral hybrid grid method, the volume grid resolution is controlled by changing adjacent surface grid resolution. Thus, it is difficult to control volume grid resolution explicitly. In body-fitted Cartesian grid method, the volume grid is generated before the surface grid generation. By using sphere-type sources, volume Cartesian cells can be refined locally as shown in Fig. 11. If all of the specified cell level is same among sources, resulting volume Cartesian cells inside the volume sources have same cell level, which is favorable to capture longitudinal vertical flows as shown in left of Fig. 11. By using body-fitted Cartesian grid method, volume and surface cells can be refined without the cell quality degeneracy. Cartesian cell can be subdivided into 8 cells by using octree data structure.

Body-fitted Cartesian grid generated near flange of rocket configuration is shown in Fig. 12. Airframe often consists of small parts, such as flange, pitot tube and so on. By using sphere-type volume sources over the flange with sufficiently small cell level specification, the computational grid is found to be successfully generated.

Another grid resolution control method is used in this study, each triangle elements of input surface can be colored based on the desired cell level. Cartesian cut cell which intersects with colored elements are refined until its cell level reaches specified resolution. This “colored geometry element grid resolution control” is used to handle narrow gap.



**Figure 11. Volume grid resolution control based on the sphere-type volume source for DLR-F6 wing-body model.**

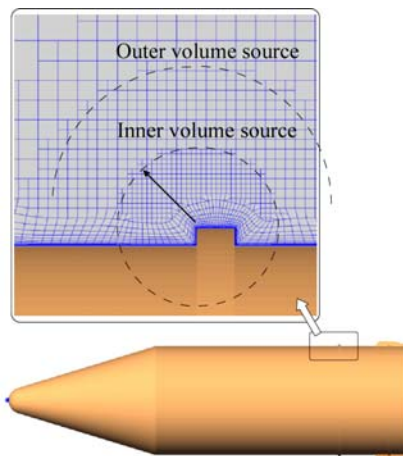


**Figure 12. Volume grid refinement based on the sphere-type volume source for rocket configuration.**

## V. Narrow Gap Treatment

In the narrow gap region layer grid thickness should be controlled to be sufficiently small value. If the layer grid thickness is appropriately controlled, valid Cartesian grid front is obtained as shown in left of Fig. 6. Cartesian grid front should cover input surface entirely to generate layer grid. In order to handle narrow gap region, geometry elements in the narrow gap region is firstly detected and listed. Then, for each listed triangle elements, sufficiently small length of the displacement vector is given to control the layer grid thickness during the ghost surface generation process. Ghost surface is generated based on the specified displacement vector length. After generating ghost surface, Cartesian cut cell which intersect with the triangle elements in the narrow gap region is refined until the cell level reaches sufficiently smaller value so that valid Cartesian grid front is obtained. Once valid Cartesian grid front is obtained, following process is the same as other geometries as shown in Fig. 7. Detailed description is given as follows for each step.

### Detection of narrow gaps

In Fig. 13, overview of the narrow gap detection procedure is shown. For each geometry element, following equation is used to identify whether the elements is in the narrow gap region or not.

$$flag1 = \left[ |\vec{V}_p| < D_{ngap} \right] \cap \left[ angle(\vec{n}_i, \vec{n}_j) < \theta_{ngap,1} \right] \cap \left[ angle(\vec{n}_i, \vec{n}_p) > \theta_{ngap,2} \right] \quad (1)$$

After this detection, elements in the situation as shown in middle figure of Fig. 13 are detected and marked for next process. Where,  $i$  is an index of the current candidate element,  $j$  is an opposite side counterpart element.  $\vec{V}_p$  is the vector between the center of element  $i$  and the closest point on the opposite side surface.  $\vec{n}_i$  and  $\vec{n}_j$  are unit normal vector of element  $i$  and  $j$ .  $D_{ngap}$  is a user-specified threshold values for the narrow gap distance.  $\theta_{ngap,1}$  and  $\theta_{ngap,2}$  are threshold values, where 120 and 45 are used as default values. If equation (1) returns TRUE, counterpart element  $j$  is marked as narrow gap element. Then, remained elements are detected by using following equation.

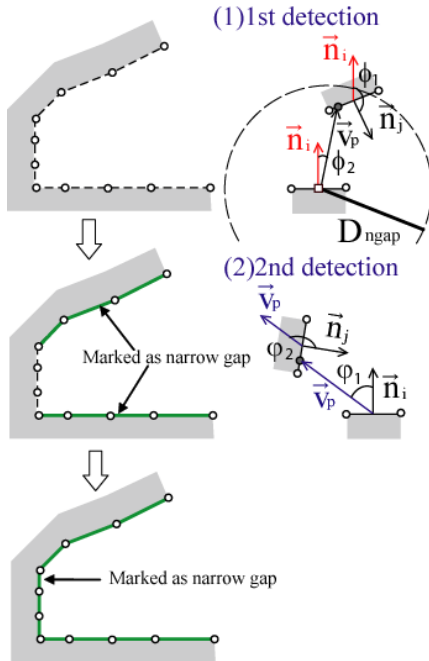


Figure 13. Narrow gap region detection algorithm.

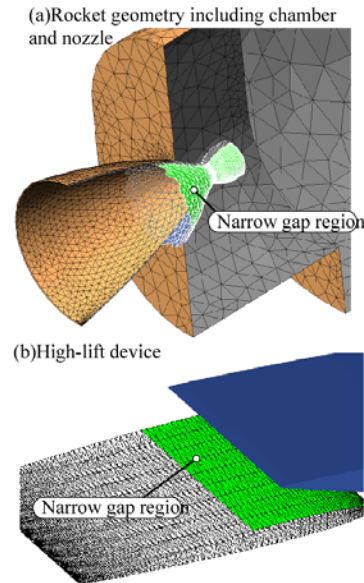


Figure 14. Detected Narrow gap region.

$$flag2 = \left[ \left| \vec{V}_p \right| < D_{ngap} \right] \cap \left[ angle(\vec{n}_i, \vec{n}_p) > \theta_{ngap,3} \right] \cap \left[ angle(\vec{n}_j, \vec{n}_p) < \theta_{ngap,4} \right]$$

$\theta_{ngap,3}$  and  $\theta_{ngap,4}$  are threshold values, where 87 and 90 are used as default values. In Fig. 14, example of the detected narrow gap elements are shown.

#### Ghost surface generation to handle narrow gap

Ghost surface is generated by the extrusion of geometry nodes toward the outside based on the displacement normal vectors on each geometry nodes on the surface. Length of the displacement vector for the narrow gap elements is specified to be small so that valid Cartesian grid front is obtained as shown in Fig. 15. Currently this length is given by the user, but this value can be intelligently calculated. This task is the future topic.

#### Cartesian grid front generation with grid resolution control in narrow gap region

Cartesian grid is generated over the ghost surface obtained in the previous step to obtain Cartesian grid front. In order to obtain valid Cartesian grid front, Cartesian cut cell which intersects with narrow gap elements on ghost surface is refined to be sufficiently small as shown in left of Fig. 15. By this treatment, valid Cartesian grid front is obtained as shown in Figs. 15 and 16. Corresponding computational grids are also shown in same figures. As shown in these figures, body-fitted Cartesian grid method is successfully extended for narrow gap problems.

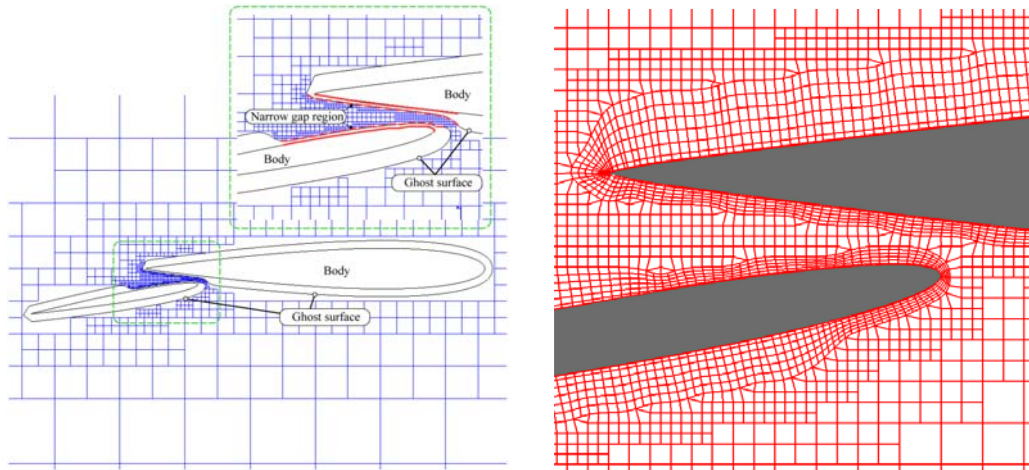


**Figure 15. Narrow gap handling and resulting grid for high lift device.**

## VI. Conclusion

In order to exploit advantages of body-fitted Cartesian grid method, an improvement of efficiency for the grid front generation, development of the explicit grid resolution control method, and an extension to narrow gap geometry were conducted. In order to obtain Cartesian grid front, the ghost surface is generated by the extrusion of the input geometry surface. Then, instead of the near-surface cell removal, Cartesian grid is generated over the ghost surface. This approach is simple and much faster than that of the previous approaches. Through the demonstration cases of DLR-F6 wing-body model, its impact on the turnaround time was confirmed to be large. By changing the displacement vector length for the ghost surface generation, the layer grid thickness can be explicitly controlled.

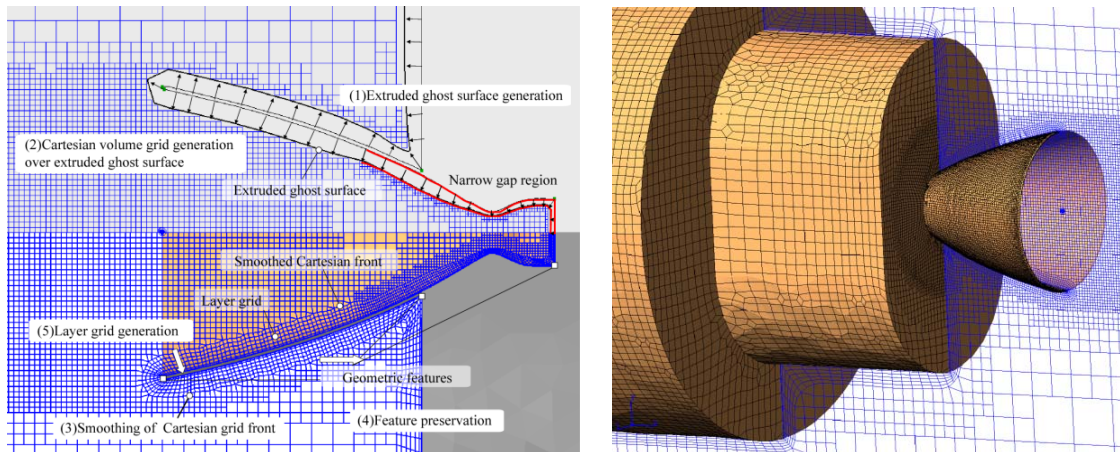


**Figure 16. Narrow gap handling for rocket configuration.**

In order to control grid resolution, sphere-type source is employed and each has desired grid resolution parameter. Cartesian cells inside the sphere are refined until its cell level reaches the specified desired grid resolution. By addition of sphere sources along the features, the grid resolution near the feature can be controlled easily.

In order to handle narrow gap geometry, narrow gap region is firstly detected based on the face normal vector information, then the length of displacement vector on the nodes of narrow gap region is specified to be sufficiently small to prevent extrusion vector collapse. Then, for all of the geometry faces in the narrow gap region, desired grid resolution length is specified appropriately to obtain valid Cartesian grid front. Through the demonstration cases of high lift device and rocket configuration, it was shown that the body-fitted Cartesian grid method was successfully extended to apply narrow gap problem.

### References

- <sup>1</sup>Nakahashi, K., "Adaptive Prismatic Grid Method for External Viscous Flow Computations," Proceedings of 11th AIAA Computational Fluid Dynamics Conference, July 1993, Orlando, FL. AIAA Paper 1993-3314.
- <sup>2</sup>Kallinderis, Y., Khawaja, A. and McMorris, H., "Hybrid Prismatic/Tetrahedral Grid Generation for Complex Geometries," AIAA Paper 1995-0210, 1995.
- <sup>3</sup>Coirier, W. J. and Jorgenson, P. C. E., "A Mixed Volume Grid Approach for the Euler and Navier-Stokes Equations," AIAA Paper 1996-0762, 1996.
- <sup>4</sup>Rogers, S. E., Roth, K., Nash, S. M., Baker, M. D., Slotnick, J. P., Whitlock, M., Cao, H. V., "Advances in Overset CFD Processes Applied to Subsonic High-Lift Aircraft," AIAA Paper 2000-4216, June 2000.
- <sup>5</sup>Karman, S. L., "SPLITFLOW: A 3D Unstructured Cartesian/Prismatic Grid CFD Code for Complete Geometries," AIAA Paper 1995-0343, 1995.
- <sup>6</sup>Wang, Z. J., "Proof of Concept - An Automatic CFD Computing Environment with a Cartesian/Prism Grid Generator, Grid Adaptor and Flow Solver", in Proceedings of 4th International Meshing Roundtable, pp 87-99, October 1995, Albuquerque, New Mexico.
- <sup>7</sup>Wang, Z. J., "A Quadtree-Based Adaptive Cartesian/Quad Grid Flow Solver for Navier-Stokes Equations," Computers & Fluids, Vol. 27, No. 4, pp.529-549, 1998.
- <sup>8</sup>Ives, D., "Geometric Grid Generation," Surface Modeling, Grid Generation, and Related Issues in Computational Fluid Dynamic (CFD) Solutions, NASA CP-3291, 1995, pp. 535-557.
- <sup>9</sup>Smith, R. J., and Leschziner, M. A., "A Novel Approach To Engineering Computations for Complex Aerodynamic Flows," Proceedings of the 5th International Conference on Numerical Grid Generation in Computational Field Simulations, Mississippi State University, MS, 1996.

- <sup>10</sup>Tchon, K. F., Hirsch, C. and Schneiders, R., "Octree-Based Hexahedral Mesh Generation for Viscous Flow Simulations," AIAA Paper 1997-1980-CP, 1997.
- <sup>11</sup>Wang, Z. J., Chen, R. F., Hariharan, N. and Przekwas, A. J., "A 2N Tree Based Automated Viscous Cartesian Grid Methodology for Feature Capturing," AIAA Paper 1999-3300-CP.
- <sup>12</sup>Lahur, P. R., "Automatic Hexahedra Grid Generation Method for Component-based Surface Geometry," AIAA Paper 2005-5242.
- <sup>13</sup>Fujimoto, K. and Fujii, K., "Study on the Automated CFD Analysis Tools for Conceptual Design of Space Transportation Vehicles," The Institute of Space and Astronautical Science (ISAS) Research Note, No. 810, July 2006.
- <sup>14</sup>Fujimoto, K. and Fujii, K., "Study on the Automated CFD Analysis Tools for Conceptual Design of Space Transportation Vehicles," proceedings of FEDSM2007-37128, 5<sup>th</sup> Joint ASME/JSME Fluids Engineering Conference, July 2007.
- <sup>15</sup>Dawes, W. N., Harvey, S. A., Fellows, S., Favaretto, C. F., and Velivelli, A., "Viscous Layer Meshes from Level Sets on Cartesian Meshes," AIAA Paper 2007-0555.
- <sup>16</sup>Kovalev, K., "Unstructured hexahedral non-conformal mesh generation," Ph.D. Dissertation, University of Brussel, Belgium, 2005.
- <sup>17</sup>Fujimoto, K. and Fujii, K., "Optimization-based Robust Feature Preserving Technique for Body-fitted Cartesian Grid Method," proceedings of 10<sup>th</sup> ISGG Conference on Numerical Grid Generation, Sep. 2007.